*11th Australasian Fluid Mechanics Conference*
*University of Tasmania, Hobart, Australia*
*14-18 December 1992*



# CONE ANGLES AND REYNOLDS STRESSES IN AN ADVERSE PRESSURE GRADIENT BOUNDARY LAYER

**I. MARUSIC and A.E. PERRY**

Dept of Mechanical & Manufacturing Engineering
University of Melbourne, Parkville, VIC 3052
AUSTRALIA

## Abstract

A comparison of the Reynolds stresses measured with a stationary and flying hot-wire is made for flow in a turbulent boundary layer on a smooth wall with streamwise pressure gradient. A cone angle is defined, based on the p.d.f. of velocity vector angles for a 90° X-wire. From these measurements it is possible to evaluate the conditions under which a stationary X-wire will give erroneous estimates of the Reynolds stresses in fields of strong turbulence intensities.

The response of the Reynolds stresses to the application of an adverse pressure gradient is discussed.

## 1 Introduction

Studies of adverse-pressure-gradient boundary layer flows has to date been somewhat restricted. The majority of previous investigations have been confined to mean-velocity studies and as a result there exists a distinct shortage of measurements of Reynolds stresses and other turbulence quantaties for varying pressure gradient conditions – all of which are important in understanding the structural features of the flow. Where turbulence measurements have been made using hot-wire anemometers, there remains the question of the accuracy of these measurements when made in fields of high turbulence intensities. Tutu & Chevray (1975) have shown that the use of X-wires can lead to large errors in the measurements of Reynolds stresses if made in regions of very high turbulence intensity — the problem relating to excessive angles made by the velocity vectors as they approach the X-wire. Perry, Lim & Henbest (1987) described this problem in terms of a critical cone angle: which represents the included angle of an imaginary cone within which all relative velocity vectors must fall if the X-wire and its calibrated formulation is to give correct values of inferred turbulence intensities.

No universal standard seems to exist when estimating the validity of X-wire measurements. For example: Nagabushana, Agarwal & Simpson (1988), in their study of separating turbulent boundary layers, accepted data as valid if the measured velocity vector angles were less than 60°, although no reason was given for this value. Perry *etal.* (1987), studying zero-pressure-gradient rough-wall turbulence questioned any results for angles exceeding nominally 20°. Their criterion was based on a study in which calibrated X-wires were shaken at known angles in a laminar free-stream flow.

In this study, the cone angle problem is investigated quantitatively using a flying hot-wire facility. The flying hot-wire, because of its bias velocity in the upstream direction, effectively reduces the relative angle of the velocity vectors which approach the X-wire. Comparisons between measured stationary and flying Reynolds stresses will determine whether the stationary measurements suffer from excessive cone angles.

The presented Reynolds stresses are also discussed with regard to the effect of adverse pressure gradient strength.

The coordinate system used throughout this paper is defined with $x$ in the streamwise direction, $y$ in the lateral direction and $z$ normal to the wall with fluctuating velocity components $u_1$, $u_2$ and $u_3$ respectively. In all cases overscores denote temporal mean values.

## 2 Cone angles

In previous studies: Perry *et al.* (1987) and Perry & Li (1989) have discussed the concept of a cone angle. The cone angle, $\theta_c$, will be defined here as the included angle in the plane of the X-wire of an imaginary cone (assumed to be symmetric as shown in figure 1) in which virtually all inferred velocity vectors fall. If $\theta_c$ exceeds what will be called the *critical cone angle* then incorrect values of inferred turbulence intensities will result. In general the value of the critical cone angle will depend on the included angle of the X-wire (which is nominally 90° for the results presented here) and the calibration formulation used in evaluating the velocity vectors. Modified calibration schemes incorporating yaw-response effects will effectively increase the critical cone angle for a X-wire system. Such schemes have been used by Browne, Antonia & Chua (1989) for jet flow, while Willmarth & Bogar (1977) also used a similar technique for near-wall boundary layer flow.

Estimating cone angles can be simply done by considering the p.d.f. of the measured velocity vector angles. The definition adopted here is outlined as follows. Firstly, an instantaneous velocity vector angle, $\theta_i$, is defined in the $(x,z)$-plane

$$\theta_i = artan(\frac{W_i}{U_i}) \tag{1}$$

where $U_i$ and $W_i$ are instantaneous total velocities in the streamwise and normal directions. The cone angle is then assumed to be given by

$$\theta_c = 2(|\mu_c| + 3\sigma_c) \tag{2}$$

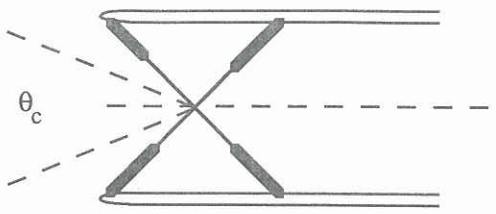


Figure 1: Symmetric cone angle in the plane of the X-wire.

where $\mu_c$ and $\sigma_c$ are the mean and standard deviation of the p.d.f. of measured velocity vector angles, $P(\theta_i)$. That is

$$\mu_c = \sum_i \theta_i P(\theta_i) \tag{3}$$

$$\sigma_c^2 = \sum_i (\theta_i - \mu_c)^2 P(\theta_i) \tag{4}$$

Typically for boundary layer flows, $\mu_c$ is small and the $\pm 3\sigma_c$ domain includes approximately 99% of the population sample.

## 3 Experimental details

Of fundamental importance to this experimental study was the need to fly a X-wire through an adverse pressure gradient boundary layer. The salient features of the design involved operating the working section of a 4.3 m long working section (940x388 mm cross-section) above atmospheric pressure. The streamwise pressure gradient was then established by using twelve louvres (which made up the roof) to control the amount and position of air being bled along the length of the working section. (The same principle was used by Clauser 1954). Each louvre was installed in two pieces, being cantilevered from both sides such that a 56 mm gap remained close to the centreline of the tunnel. This slot allowed room for the 'sting' of the flying hot-wire mechanism to pass through and travel along the length of the working section. The flying hot-wire mechanism is essentially as described by Watmuff, Perry & Chong (1983). In order to avoid significant secondary flows being induced by the presence of the slot, specially fared sealing gates were built and were opened and closed smoothly using a prying mechanism which was mounted around the hot-wire sting. Overall, the system ran quite smoothly and could comfortably accomodate a flying speed of 3 m/s. Full details of the flying mechanism and the wind tunnel design are given by Marusic (1991).

All turbulence measurements were made with X-wires constructed with 5 $\mu$m diameter platinum Wollaston wire, etched nominally to 1.0 mm. The wires were separated by a distance of 1.0 mm and were nominally attached at $\pm 45^o$ to the streamwise direction. The X-wire probe was held in a chuck which allowed accurate rotation through $90^o$, enabling measurements to be taken in both the $(x,z)$- and $(x,y)$-planes. Constant temperature hot-wire anemometers were used for all measurements and were operated at a resistance ratio of 2.0. The anemometry and the non-linear dynamic calibration procedure used in the study are close to those described in Perry (1982). Signals were sampled on-line to a PC using a 12-bit A-D converter. For the broadband turbulence measurements, the hot-wire signals were low-pass filtered at 15.8 kHz. In order to get convergence of the Reynolds stresses: 32000 samples were taken at a rate of 200 Hz for the stationary case, while for the flying measurements 60000 samples were taken at a rate of approximately 3000 Hz (determined by flying speed) over a 55 mm range about the measuring station. (This corresponded to 1000 sled passes). See Marusic (1991) for full details.

## 4 Results

The flow case being considered had an upstream velocity, $U_\infty$, set nominally to 10 m/s. The pressure gradient distribution is shown in figure 2.

Here $C_p \equiv 2(P - P_\infty)/\rho U_\infty^2 = 1 - (U_1/U_\infty)^2$ where $P$ and $U_1$ are the static pressure and free-stream velocity respectively, at streamwise distance $x$. The boundary layer flow is seen to be initially in a zero pressure gradient condition which is then acted upon by an approximately constant adverse pressure gradient. Figure 2 also shows the location of the measuring stations where all turbulence measurements were made. Table 1 gives further information obtained from mean-flow measurements for these measuring stations. The boundary layer is noted as being in a rapidly developing state and consequently is not in any way close to being a quasi-equilibrium flow. (Such flows have made up the large majority of previous adverse-pressure-gradient studies).

The cone angles measured at each of the stations for both the $(x,z)$- and $(x,y)$-planes are shown in figure 3. A consistent trend is observed with $\theta_c$ increasing for increasing values of Coles' wake factor $\Pi$. (Here $\Pi$ is directly related here to increasing adverse pressure gradient strength – see table 1). Also, the cone angles in the $(x,y)$-plane are seen to be typically more than $10^o$ larger as compared to the $(x,z)$-plane – reflecting the larger turbulence intensities occuring in this plane.

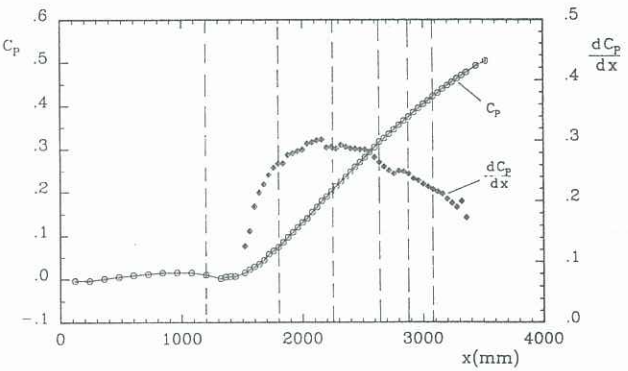


Figure 2: Streamwise pressure distribution. Dashed lines indicate the position of measuring stations.

| $x$ (mm) | $\Pi$ | $\beta_x$ | $R_\theta$ |
|---|---|---|---|
| 1200 | 0.42 | $\approx 0.0$ | 2206 |
| 1800 | 0.68 | 0.650 | 3153 |
| 2240 | 1.19 | 1.453 | 4155 |
| 2640 | 1.87 | 2.899 | 5395 |
| 2880 | 2.46 | 4.484 | 6395 |
| 3080 | 3.23 | 7.160 | 7257 |

Table 1: $\Pi$ is Coles' wake factor; $\beta_x = (\delta^*/\tau_o)(dP/dx)$ where $\delta^*$ is displacement thickness and $\tau_o$ is wall shear stress. $R_\theta$ is Reynolds number based on momentum thickness.

Corresponding measurements of the turbulence intensities and the Reynolds shear stresses, made with both stationary and flying hot-wires are shown in figure 4. The results indicate that in the $(x, z)$-plane, where the cone angles are all less than 45°, no significant differences between the flying and stationary measurements are observed. It is noted however, that some evidence of a difference was beginning to occur for the $x = 3080$ mm station. In the $(x, y)$-plane, where some profiles had cone angles in excess of 50°, the $\overline{u_2^2}$ measurements show clear differences between the flying and stationary measurements. The difference is beyond any estimated errors in measuring $\overline{u_2^2}$ as determined from the dynamic calibration procedure. Therefore the stationary measurements are concluded to be suffering from cone-angle problems and consequently under-estimate the true turbulence intensities.

From the results it would seem that the critical cone angle for the X-wire and its calibration formulation is approximately $40 - 45°$. All measurements with cone angles above this value would seem to result in an underestimation of corresponding turbulence quantities. A more decisive estimate could be obtained by studying flows with higher turbulence intensities — such as in separating flows.

In order to determine if the flying stress measurements are in fact correct, a check of the flying hot-wire cone angles is required to ensure that they are below the critical cone angle. (If this is not the case then the flying velocity of the sled would need to be increased). Figure 5 shows the flying cone angles taken in the (x,y)-plane at $x = 3080$ mm. Reassuringly all angles are seen to be well below the critical cone angle threshold. Figure 6 illustates how the p.d.f's of the velocity angles compare for a typical flying and stationary case.

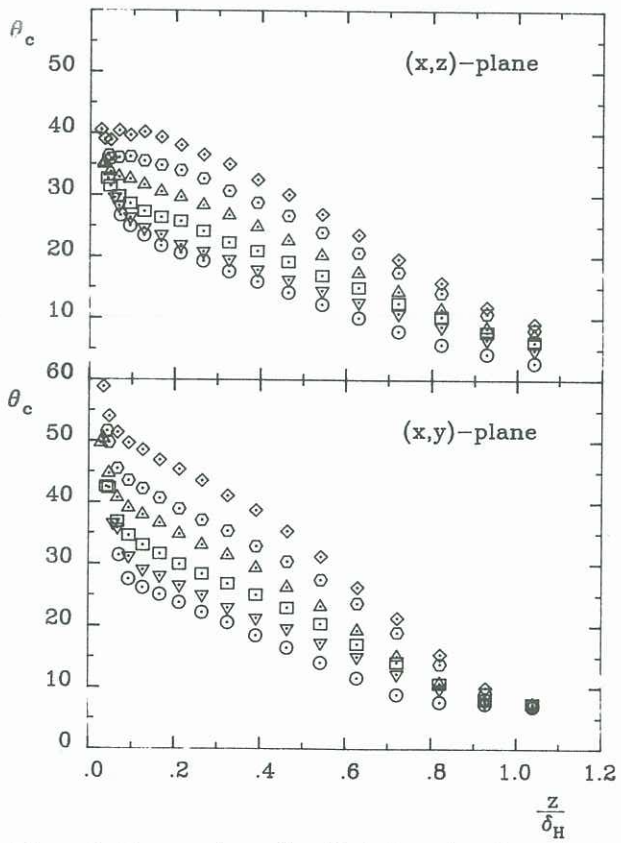


Figure 3: Cone angle profiles.($\delta_{II}$ is boundary layer thickness). Symbols as in figure 4.

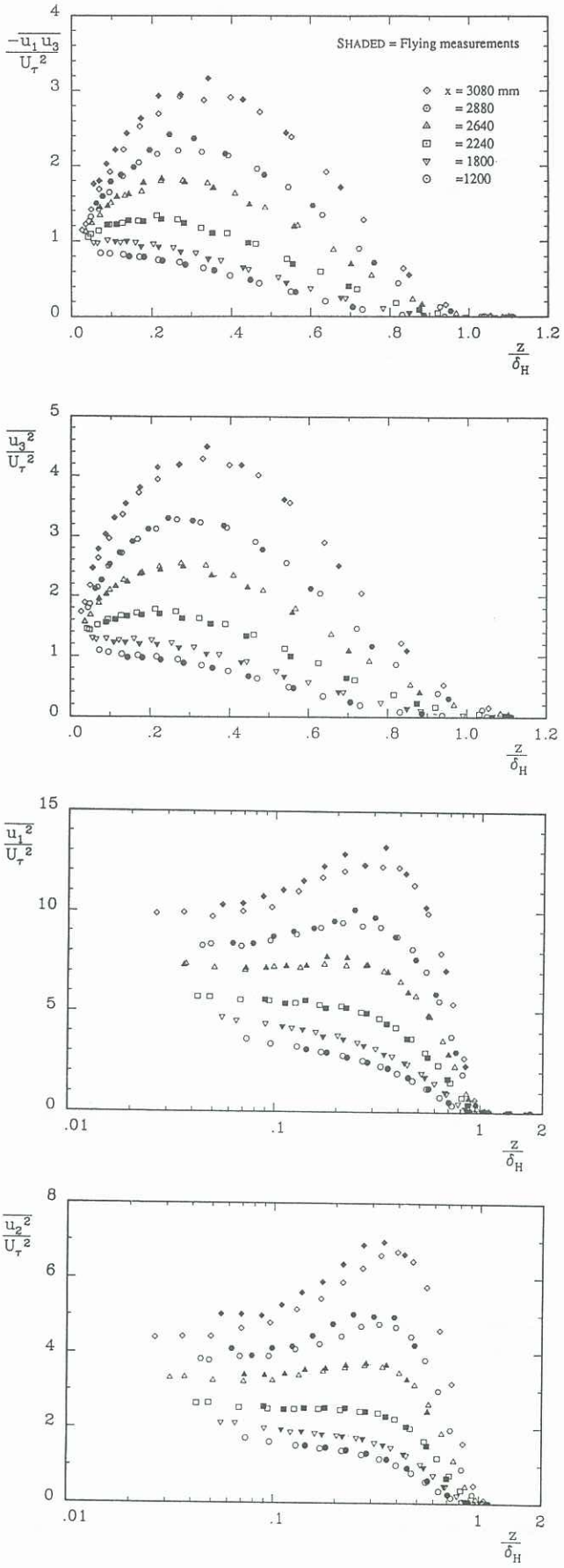


Figure 4: Reynolds stress profiles – flying (shaded) and stationary.

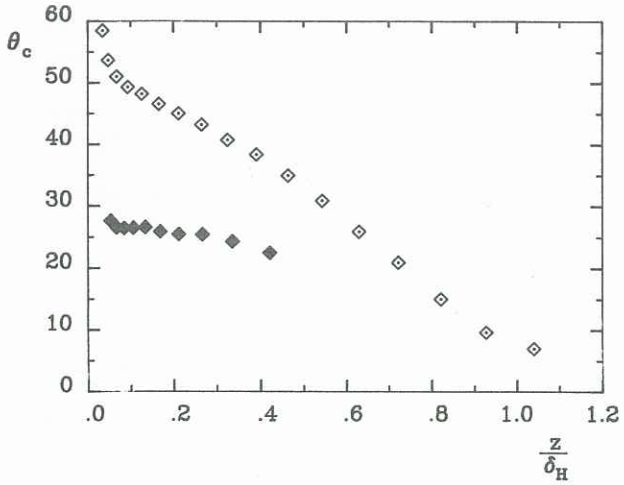


Figure 5: Comparison of flying (shaded) and stationary cone angles for x = 3080mm; (x,y)-plane.

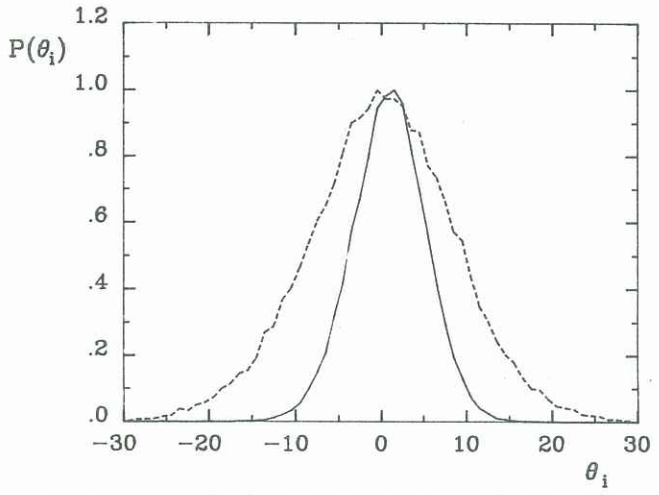


Figure 6: P.d.f.'s of the velocity vector angles for $z/\delta_H$ = 0.069 stationary (dashed line) and $z/\delta_H$ = 0.053 flying (solid line), x = 3080mm; (x,y)-plane.

## 5 Discussion

The nature of the flow being studied is such that it is essentially in a zero pressure gradient condition which is then perturbed by an almost constant adverse pressure gradient. The structure of zero pressure gradient flow is reasonably well understood in contrast to the understanding of adverse pressure gradient flows. Perry *et al.* (1987) and Perry & Li (1990) have shown the applicability of the attached eddy hypothesis in helping explain the structural features of zero pressure gradient flow. The results shown in figure 4 show how the broadband turbulence intensities and the Reynolds shear stresses change from the zero pressure gradient condition. All the components show a similar trend in that as the pressure gradient becomes strong, maximum values of the turbulence intensities occur away from the wall. The $\overline{u_3^2}$ and $-\overline{u_1u_3}$ profiles show overall trends which are very similar to each other. In the case of the strongest pressure gradient the two profiles are seen to be very similar in shape. The $\overline{u_1^2}$ and $\overline{u_2^2}$ profiles, on the other hand, show overall trends which are similar to each other. The near-wall behaviour of these two sets of profiles is seen to be very different to the $\overline{u_3^2}$ and $-\overline{u_1u_3}$ profiles. For the strongest pressure gradients, the $\overline{u_3^2}$ and $-\overline{u_1u_3}$ profiles always increase in intensity as $z/\delta_H$ increases from the wall, until the maximum is reached. For the $\overline{u_1^2}$ and $\overline{u_2^2}$ cases, in some profiles the initial turbulence intensities decrease with increasing $z/\delta_H$ from the wall and then begin to increase again after a short distance. This behaviour is yet to be fully understood and has also been noted in other attached adverse-pressure-gradient flows, see for example East, Sawyer & Nash (1979) and Watmuff & Westphal (1989). A possible explanation being investigated involves the return of the $\overline{u_1^2}$ and $\overline{u_2^2}$ profiles at low $z/\delta_H$ levels to logarithmic-linear distributions as predicted by the attached eddy hypothesis — see Marusic (1991). In these studies however, the attached eddy hypothesis is shown to be unsuccessful in predicting the outer region behaviour of $\overline{u_1^2}$ and $\overline{u_2^2}$ when using simple attached eddies alone. These findings further illustrate the structural differences between adverse pressure gradient and zero pressure gradient flow. These issues remain the subject of a continuing investigation by the authors.

## 6 Conclusions

A flying hot-wire was used to investigate the cone angle problem for 90° X-wires in a turbulent boundary layer with adverse pressure gradient. It was generally found that the cone angles measured in the (x,y)-plane were typically 10° larger than compared to the (x,z)-plane. By measuring the corresponding Reynolds stresses with both stationary and flying X-wires, it was found that when the cone angle exceeded nominally 40–45° an error in the stationary wire measurements occured. This error caused an underestimation of the true Reynolds stress.

The behaviour of the Reynolds stresses, originally in a zero pressure gradient condition, were examined in response to an approximately constant adverse pressure gradient being applied. The behaviour of the $\overline{u_1^2}$ and $\overline{u_2^2}$ profiles for large $\Pi$ values is noted as containing additional information which existing versions of the attached eddy hypothesis model are unable to account for.

The authors wish to acknowlegde the financial assistance of the Australian Research Council.

## References

Browne, L. W. B., Antonia, R. A. & Chua, L. P. (1989) *Exp. Fluids.* **7**, 201.

Clauser, F. H. (1954) *J. Aeronautical Sci.* Feb.

East, L. F., Sawyer, W. G. & Nash, C. R. (1979) *R.A.E. TR-79040.*

Marusic, I. (1991) Ph.D. thesis, University of Melbourne, Australia.

Nagabushana, K. A., Agarwal, N. K. & Simpson, R. L. (1988) *AIAA-88-0616.*

Perry, A. E. (1982) *Hot-Wire Anemometry.* Claredon Press, Oxford University.

Perry, A. E., Lim, K. L. & Henbest, S. M. (1987) *J. Fluid Mech.* **177**, 437.

Perry, A. E. & Li, J. D. (1990) *J. Fluid Mech.* **218**, 405.

Tutu, N. K. & Chevray, R. (1975) *J. Fluid Mech.* **71**, 785.

Watmuff, J. H., Perry, A. E. & Chong, M. S. (1979) *Exp. Fluids.* **1**, 63.

Willmarth, W. W. & Bogar, T. J. (1977) *Phys. Fluids* **20**, S9.